Journal of Materials Science: Materials in Electronics
https://doi.org/10.1007/s10854-018-8599-x

Crystal structure, microstructure and microwave dielectric properties of novel $MgAl_2Ti_3O_{10}$ ceramic

Huanfu Zhou[1] · Wendong Sun[1] · Jin Huang[1] · Kangguo Wang[1] · Xiuli Chen[1] · Xiaobin Liu[1] · Hong Ruan[1]

Received: 19 December 2017 / Accepted: 12 January 2018

Abstract

In the present work, a novel $MgAl_2Ti_3O_{10}$ ceramic was obtained using a traditional solid-state reaction method. X-ray diffraction and energy dispersive spectrometer showed that the main $MgAl_2Ti_3O_{10}$ phase was formed after sintered at 1300–1450 °C. With rising the sintering temperature from 1300 to 1450 °C, the bulk density (ρ), relative permittivity (ε_r) and $Q\times f$ value firstly increased, reached the maximum values (3.61 g/cm^3, 14.9, and 26,450 GHz) and then decreased. The temperature coefficient of resonator frequency (τ_f) showed a slight change at a negative range of − 94.6 to − 83.7 ppm/°C. When the sintering temperature was 1400 °C, $MgAl_2Ti_3O_{10}$ ceramics exhibited the best microwave dielectric properties with $Q\times f = 26{,}450$ GHz, $\varepsilon_r = 14.9$ and $\tau_f = -83.7$ ppm/°C.

1 Introduction

With the rapid development of mobile communication, the demands for electronic devices with high frequency, lightweight and low cost are sharp increasing. To meet the above requirements, low permittivity, high $Q\times f$ value and near-zero τ_f are necessary to microwave components [1–5]. It is well known that the microwave dielectric materials have the function of division, transmission and resonance in the circuit [6–8]. In recent years, many ceramic systems with good microwave dielectric properties have been explored, such as Ba(X, Y)O_3 (X = Zn, Mg, Y = Nb, Ta) [9], (Zr, Sn)TiO_4 [10] and BaO–TiO_2 [11], but high costs of raw materials restricted their further applications. Kagata et al. [12] reported that a ternary system with composition of Al_2O_3–MgO–ReO_x (Re: rare earth) exhibited low permittivity and near-zero τ_f. Nevertheless, high-cost raw materials also limited its commercial applications. So, more works are focusing on searching for novel material systems with low cost of raw materials.

Bridge et al. [13] reported that MgO–Al_2O_3–TiO_2 ceramic system exhibited low cost of raw materials, which were the most common microwave materials used in ceramics packaging. Cordierite ceramics with low permittivity and dielectric loss, high chemical and thermal stability are in accordance with the directions of miniaturization, so more and more novel ceramic materials have been widely researched and applied in recent years [14–16]. In this work, $MgAl_2Ti_3O_{10}$ ceramics were obtained by the traditional solid-state reaction (SSR) method. Furthermore, the phase composition, microstructure and microwave dielectric properties of ceramics were also studied.

2 Experimental procedure

$MgAl_2Ti_3O_{10}$ ceramics were prepared by the SSR method using high purity raw material of MgO (≥ 98.5%), Al_2O_3 (≥ 99%) and TiO_2 (≥ 99%). In order to remove the moisture of MgO, the crude material was calcined at 800 °C for 2 h. Raw materials were weighed on the basis of the ratio with MgO:Al_2O_3:TiO_2 = 1:1:3 and ball-milled for 4 h via absolute ethanol and zirconium ball. After drying, the mixtures were calcined at 1200 °C for 4 h. Next, the calcined powders were secondary ball-milled with the method described above. After adding 5 wt% polyvinyl alcohol (PVA), the granular powders were uniaxially pressed into columns with

✉ Huanfu Zhou
zhouhuanfu@163.com

1 Guangxi Ministry-Province Jointly-Constructed Cultivation Base for State Key Laboratory of Processing for Non-ferrous Metal and Featured Materials, Guangxi Key Laboratory in Universities of Clean Metallurgy and Comprehensive Utilization for Non-ferrous Metals Resources, Collaborative Innovation Center for Exploration of Hidden Nonferrous Metal Deposits and Development of New Materials in Guangxi, School of Materials Science and Engineering, Guilin University of Technology, Guilin 541004, China

Published online: 17 January 2018

12 mm in diameter and 6 mm in thickness under the pressure of 200 MPa. In addition, the samples were heated to 550 °C at a rate of 1 °C/min for 4 h to remove the organic binders. Finally, the samples were sintered at 1300–1450 °C for 4 h.

The phase structure was analyzed by an X-ray diffraction (XRD) with CuK$_α$ radiation generated at 40 kV and 40 mA (Model X'Pert PRO, PANalytical, Almelo, Holland). The morphology of ceramics was studied by a scanning electron microscopy (SEM) (Model JSM6380-LV SEM, JEOL, Tokyo, Japan), and the elemental analysis was conducted on the energy dispersive spectrometer (EDS) (Model IE 350, INCA, Oxford, U.K.). The Archimedes method was used to measure the bulk densities of ceramic samples. A Network Analyzer (Model E5071C, Agilent Co., CA, 300 kHz–20 GHz) with the $TE_{01\delta}$ shielded cavity method was used to measure the relative permittivity (ε_r) and quality factor ($Q \times f$). Then the samples were put into a temperature chamber (DELTA9039, Delta Design, USA) one by one, and the resonant frequency in the temperature range of 25–85 °C was measured by the Network Analyzer mentioned above. The temperature coefficient of resonant frequency (τ_f) was calculated by the following formula:

$$\tau_f = \frac{f_T - f_0}{f_0(T - T_0)} \tag{1}$$

where f_T, f_0 are the $TE_{01\delta}$ resonant frequencies at temperature T (85 °C) and T_0 (25 °C), respectively.

3 Results and discussion

Figure 1 demonstrates the XRD patterns of the $MgAl_2Ti_3O_{10}$ ceramics sintered at 1300–1450 °C. It can be seen that $MgAl_2Ti_3O_{10}$ ceramics mainly generated $MgAl_2Ti_3O_{10}$ phase (PDF#00-005-0450). Besides, small amount of TiO_2 and Al_2O_3 phases were detected in the XRD patterns due to the inadequate reaction. With increasing the sintering temperature from 1300 to 1400 °C, the diffraction peaks of the second phases declined slightly. However, when the sintering temperature further increased to 1425 °C, the second phases increased due to over-sintering of ceramics. The next work will obtain a pure phase by nonstoichiometry [17].

Figure 2 shows the SEM images of the $MgAl_2Ti_3O_{10}$ ceramics sintered at different temperatures. With increasing the sintering temperature from 1300 to 1400 °C, the grain size of ceramics increased gradually. Especially, when the temperature reached 1400 °C, the best crystallinity of the ceramics was obtained and the particle size was homogeneous. However, it due to over-sintering, the abnormal grain growth and crack occurred with further increasing the sintering temperature [18]. EDS analysis of the $MgAl_2Ti_3O_{10}$ ceramics sintered at 1400 °C was listed in Table 1. EDS is performed on the small and large grain regions [19]. From the data of EDS analysis, Mg, Al and Ti could be discovered in the part "I" and "II", and the ratio between atoms was close to 1:2:3. The result indicates that the crystalline phase of ceramics is really $MgAl_2Ti_3O_{10}$ phase.

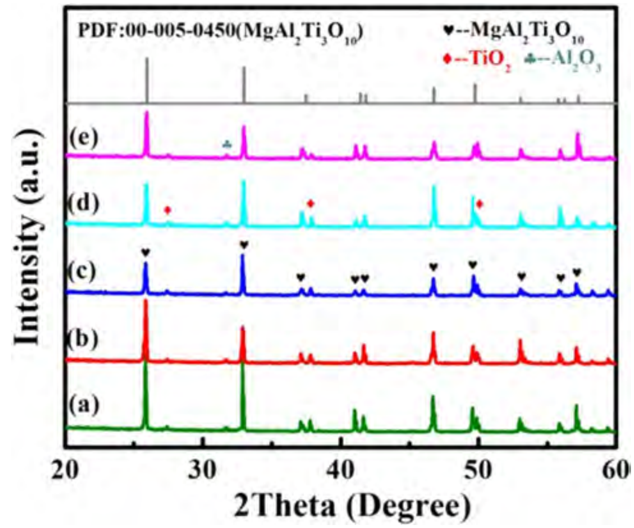

Fig. 1 XRD patterns of $MgAl_2Ti_3O_{10}$ ceramics sintered at: (*a*) 1300 °C, (*b*) 1350 °C, (*c*) 1400 °C, (*d*) 1425 °C, (*e*) 1450°C

Figure 3 illustrates the bulk density (ρ), relative permittivity (ε_r), quality factor ($Q \times f$) and temperature coefficient of resonator frequency (τ_f) for $MgAl_2Ti_3O_{10}$ ceramics sintered at different temperatures. With increasing the sintering temperature, the ρ of $MgAl_2Ti_3O_{10}$ ceramics firstly increased and then decreased slowly. The maximum value of bulk density ~3.61 g/cm^3 appeared at 1400 °C. Nevertheless, when the temperature rose to 1450 °C, the ρ declined to 3.60 g/cm^3. The ε_r is related to the material compositions, grain size and the density of ceramics [20]. In other words, the ε_r is affected by the ρ of ceramics. When the sintering temperature increased to 1400 °C, the ε_r increased to 14.9. However, when the sintering temperature continued to increase to 1425 °C, the ε_r decreased gradually because excessive sintering temperature resulted in the abnormal grain growth and cracks [21], as shown in Fig. 2.

The $Q \times f$ values of $MgAl_2Ti_3O_{10}$ ceramics have a close relationship with the bulk density. With consistently increasing the sintering temperature, the microstructure of the samples has become denser and the grain grew up gradually and the content of second phases declined slightly, so the quality factor of ceramics increased. When the sintering temperature increased from 1300 to 1400 °C, the $Q \times f$ values increased

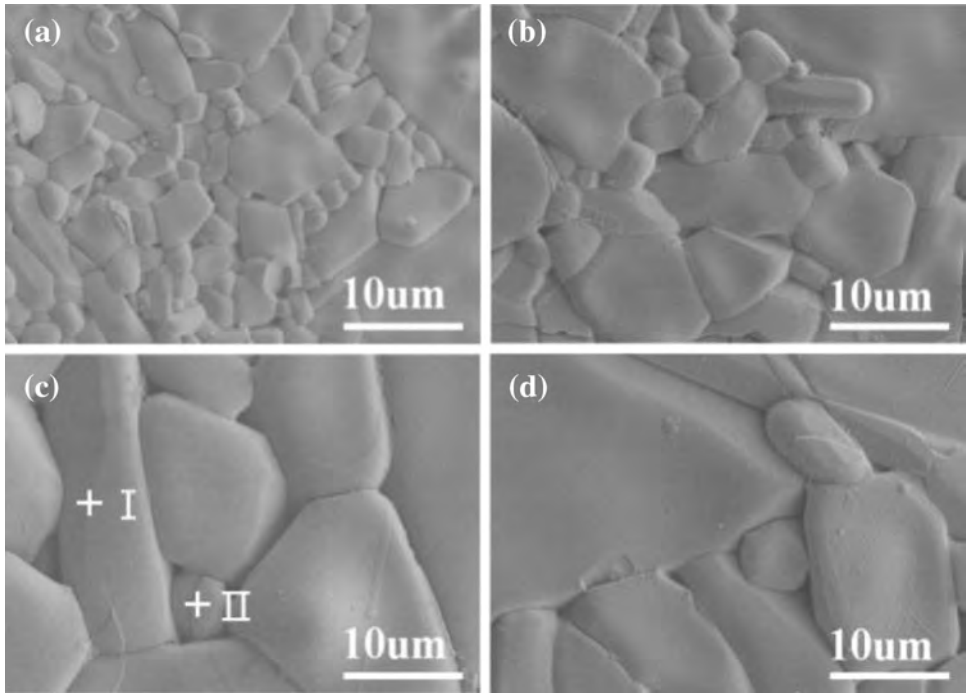

Fig. 2 SEM images of $MgAl_2Ti_3O_{10}$ ceramics sintered at: (*a*) 1300 °C, (*b*) 1350 °C, (*c*) 1400 °C, (*d*) 1450°C

Table 1 EDS analysis of $MgAl_2Ti_3O_{10}$ ceramics sintered at 1400°C

Region	Atomic (%)			
	Mg K	Al M	Ti K	O K
I	6.12	10.72	14.85	68.31
II	6.19	10.64	13.85	69.31

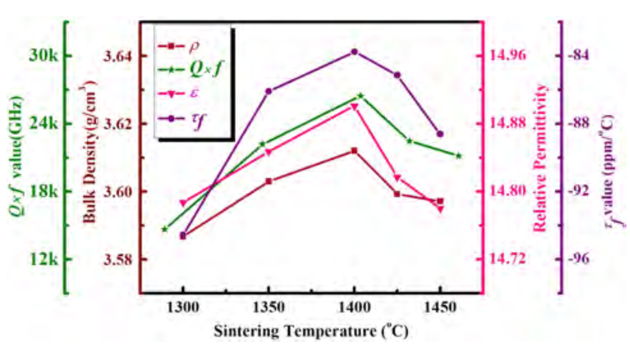

Fig. 3 Bulk density, relative permittivity, $Q \times f$ and τ_f of $MgAl_2Ti_3O_{10}$ ceramics as a function of the sintering temperature

from 14,670 to 26,450 GHz. With further increasing the sintering temperature, the $Q \times f$ values decreased due to the increase of the second phases, abnormal grain growth and cracks. Especially, when the sintering temperature rose to 1450 °C, the $Q \times f$ value declined to 21,130 GHz. It is well known that the τ_f is related to the composition of materials [22–24]. Because there was not obvious change in composition of samples, the τ_f of $MgAl_2Ti_3O_{10}$ ceramics maintained at a negative range (−94.6 to −83.7 ppm/°C). The microwave dielectric properties between the relate material systems and our work are listed in Table 2. Compared with $Mg_3Nb_4Al_{44}O_{75}$, 3CaO–2ZnO–Ta_2O_5–TiO_2 [25], $MgCu_2Nb_2O_8$ [26] and $ZnMnW_2O_8$ [27] systems, $MgAl_2Ti_3O_{10}$ ceramic obviously exhibited high $Q \times f$ value and low cost of raw materials, indicating that it is a candidate for microwave devices.

4 Conclusion

$MgAl_2Ti_3O_{10}$ ceramics have been prepared by the traditional SSR method. The main phase of $MgAl_2Ti_3O_{10}$ was formed along with small amount of TiO_2 and Al_2O_3. When the sintering temperature reached 1400 °C, $MgAl_2Ti_3O_{10}$ ceramics exhibited high crystallinity and uniform granularity. With increasing the sintering temperature, the ε_r, $Q \times f$ values and τ_f of $MgAl_2Ti_3O_{10}$ ceramics match the change rules of bulk density. When the sintering temperature was 1400 °C, $MgAl_2Ti_3O_{10}$ ceramics exhibited good properties with $Q \times f = 26{,}450$ GHz, $\varepsilon_r = 14.9$ and $\tau_f = -83.7$ ppm/°C.

Table 2 Microwave dielectric properties between $MgAl_2Ti_3O_{10}$ ceramic and several ceramic compositions

Ceramic composition	Sintering temperature (°C)	ε_r	$Q\times f$ (GHz)	τ_f (ppm/°C)	Ref.
$Mg_3Nb_4Al_{44}O_{75}$	1680	15.0	11,000	35.0	[24]
$3CaO–2ZnO–Ta_2O_5–TiO_2$	1325	16.0	34,500	− 49.0	[24]
$MgCu_2Nb_2O_8$	1010	15.9	6780	− 46.0	[25]
$ZnMnW_2O_8$	950	13.7	10,670	− 17.0	[26]
$MgAl_2Ti_3O_{10}$	1400	14.9	26,450	− 83.7	Our work

Acknowledgements This work was supported by Natural Science Foundation of China (Nos. 11464009, 61761015, 11664008 and 11364012), Natural Science Foundation of Guangxi (Nos. 2017GXNSFDA198027, 2015GXNSFDA139033 and 2017GXNSFFA198011).

References

1. J.T. Zhang, S.Q. Xu, D.X. Zhou, Development of microwave dielectric materials and its applications. Electron. Compon. Mater. **23**, 6–9 (2004)
2. Z.Y. Zou, Z.H. Chen, X.K. Lan, W.Z. Lu, B. Ullah, X.H. Wang, W. Lei, Weak ferroelectricity and low-permittivity microwave dielectric properties of $Ba_2Zn_{(1+x)}Si_2O_{(7+x)}$ ceramics. J. Eur. Ceram. Soc. **37**, 3065–3071 (2017)
3. L.X. Pang, D. Zhou, W.G. Liu, Low-temperature sintering and microwave dielectric properties of $CaMo_4$-based temperature stable LTCC material. J. Am. Ceram. Soc. **97**, 2032–2034 (2014)
4. H.F. Zhou, J. Huang, X.H. Tan, Microwave dielectric properties of low-permittivity $CaMgSiO_4$ ceramic. J. Mater. Sci. Mater. Electron. **28**, 15258–15262 (2017)
5. X.K. Lan, Z.Y. Zou, W.Z. Lu, J.H. Zhu, W. Lei, Phase transition and low-temperature sintering of $Zn(Mn_{1-x}Al_x)_2O_4$ ceramics for LTCC applications. Ceram. Int. **42**, 17731–17735 (2016)
6. Q.L. Zhang, H. Yang, H.P. Sun, A new microwave ceramic with low-permittivity for LTCC applications. J. Eur. Ceram. Soc. **28**, 605–609 (2008)
7. W. Lei, W.Z. Lu, X.H. Wang, F. Liang, J. Wang, Phase composition and microwave dielectric properties of $ZnAl_2O_4–Co_2TiO_4$ low-permittivity ceramics with high quality factor. J. Am. Ceram. Soc. **94**, 20–23 (2011)
8. C.C. Xia, D.H. Jiang, G.H. Chen, Y. Luo, Microwave dielectric ceramic of $LiZnPO_4$ for LTCC applications. J. Mater. Sci. Mater. Electron. **28**, 12026–12031 (2017)
9. W.C. Tzou, Y.S. Yang, C.F. Yang, Microstructure and microwave dielectric characteristics of $(1-x)Ba(Zn_{1/3}Ta_{2/3})O_3–xBaTi_4O_9$ ceramics. Mater. Res. Bull. **42**, 1897–1904 (2007)
10. T. Takada, S.F. Wang, S. Yoshikawa, Effects of glass additions on (Zr, Sn)TiO_4 for microwave applications. J. Am. Ceram. Soc. **77**, 2485–2488 (2010)
11. G.H. Jonker, W. Kwestroo, The ternary systems $BaO–TiO_2–SnO_2$ and $BaO–TiO_2–ZrO_2$. J. Am. Ceram. Soc. **41**, 390–394 (2010)
12. H. Kagata, R. Saito, H. Katsumura, $Al_2O_3–MgO–ReO_x$ (Re = rare earth) based LTCC and its applications to multilayer non-shrinkage substrate for microwave devices. J. Electroceram. **13**, 277–280 (2004)
13. D.R. Bridge, D. Holland, P.W. McMillan, Development of the alpha-cordierite phase in glass ceramics for use in electronic devices. Glass Technol. **26**, 286–292 (1985)
14. J.D. Hodge, Microstructure development in mullite-cordierite ceramics. J. Am. Ceram. Soc. **72**, 1295–1298 (1989)
15. S.H. Wang, D. Zhou, Z.X. Hou, M.H. Wang, Low-temperature sintering, low-dielectric cordierite ceramic tapes for high frequency application. Ceram. Int. **39**, 9505–9509 (2013)
16. S. Wu, K.X. Song, P. Liu, H.X. Lin, F.F. Zhang, Effect of TiO_2 doping on the structure and microwave dielectric properties of cordierite ceramics. J. Am. Ceram. Soc. **98**, 1842–1847 (2015)
17. Q.S. Cao, W.Z. Lu, Z.Y. Zou, Phase compositions and reaction models of zinc manganese oxides with different Zn/Mn ratios. J. Alloy. Compd. **661**, 196–200 (2016)
18. D.R. Askins, A study of overheat damage to structural composites. Int. SAMPE Tech. Conf. **24**, T806–T820 (1992)
19. P.Q. Xu, H.Y. Gong, G.X. Xu, Study on microstructure and properties of Ni-based alloy/Y_2O_3-deposited metals by laser cladding. J. Mater. Sci. **43**, 1559–1567 (2008)
20. H.F. Zhou, X.H. Tan, J. Huang, Sintering behavior, phase structure and adjustable microwave dielectric properties of $Li_2O–MgO–nTiO_2$ ceramics ($1 \le n \le 5$). J. Mater. Sci. Mater. Electron. **28**, 6475–6480 (2017)
21. B.S. Kim, E.S. Lim, J.H. Lee, Effect of Bi_2O_3 content on sintering and crystallization behavior of low-temperature firing $Bi_2O_3–B_2O_3–SiO_2$ glasses. J. Eur. Ceram. Soc. **27**, 819–824 (2007)
22. M. Guo, G. Dou, S.P. Gong, D.X. Zhou, Low-temperature sintered $MgWO_4–CaTiO_3$ ceramics with near-zero temperature coefficient of resonant frequency. J. Eur. Ceram. Soc. **32**, 883–890 (2012)
23. H.S. Park, K.H. Yoon, Relationship between the band valence and the temperature coefficient of the resonant frequency in the complex perovskite $(Pb_{1-x}Ca_x)[Fe_{0.5}(Nb_{1-y}Ta_y)_{0.5}]O_3$. J. Am. Ceram. Soc. **84**, 99–103 (2001)
24. S. Chen, S.R. Zhang, X.H. Zhou, Low temperature preparation of the Zn_2SiO_4 ceramics with the addition of BaO and B_2O_3. J. Mater. Sci. Mater. Electron. **22**, 1274–1281 (2011)
25. P.V. Bijumon, M.T. Sebastian, P. Mohanan, Experimental investigations and three dimensional transmission line matrix simulation of $Ca_{5-x}A_xB_2TiO_{12}$ (A = Mg, Zn, Ni and Co; B = Nb and Ta) ceramic resonators. J. Appl. Phys. **98**, 526 (2005)
26. R.C. Pullar, C. Lai, F. Azough, R. Freer, N.M. Alford, Novel microwave dielectric LTCCs based upon V_2O_5 doped $M^{2+}Cu_2Nb_2O_8$ compounds (M^{2+} = Zn, Co, Ni, Mg and Ca). J. Eur. Ceram. Soc. **26**, 1943–1946 (2006)
27. J.S. Kim, J.C. Lee, C.I. Cheon. H.J. Kang, Crystal structures and low temperature cofiring ceramic property of $(1-x)$(Li, Re)$W_2O_8–xBaWO_4$ ceramics (Re = Y, Yb). Jpn. J. Appl. Phys. **45**, 7397–7400 (2006)